

¹ HydrAMP: a deep generative model for antimicrobial peptide discovery

² Paulina Szymczak^{1,†}, Marcin Mozejko^{1,†}, Tomasz Grzegorzek¹, Marta Bauer², Damian Neubauer²,
³ Michał Michalski³, Jacek Sroka¹, Piotr Setny³, Wojciech Kamysz², and Ewa Szczurek^{1,*}

⁴ *¹Faculty of Mathematics, Informatics and Mechanics, University of Warsaw*

⁵ *²Medical University of Gdańsk*

⁶ *³The Centre of New Technologies, University of Warsaw*

⁷ *[†]These authors contributed equally to this work*

⁸ *^{*}Correspondence should be addressed to szczurek@mimuw.edu.pl*

⁹ **Abstract**

Antimicrobial peptides (AMP) emerge as compounds that can alleviate the global health hazard of antimicrobial resistance. Since the repertoire of experimentally verified AMPs is limited, there is a need for novel computational approaches to peptide generation. For such approaches, exploring the amino-acid peptide representation space is infeasible due to its sparsity and combinatorial complexity. Thus, we propose HydrAMP, a conditional variational autoencoder that learns a lower-dimensional and continuous space of peptides' representations and captures their antimicrobial properties. HydrAMP outperforms other approaches in generating peptides, either *de novo*, or by analogue discovery, and leverages parameter-controlled creativity. The model disentangles the latent representation of a peptide from its antimicrobial conditions, allowing for targeted generation. Wet-lab experiments and molecular dynamics simulation confirm the increased activity of a Pexiganan-based analogue produced by HydrAMP. HydrAMP proposes new promising AMP candidates, enabling progress towards a new generation of antibiotics.

20 1 Introduction

21 Microbes pose a continuously increasing threat to human health, in particular by causing sepsis, post-surgical infec-
22 tions, and putting at risk patients with chronic conditions or immunodeficiency [1]. It is estimated that microbial
23 infection will become the main cause of death by 2050, exceeding the currently dominating cancer and cardiovascular
24 diseases [2]. The reason for the growing danger of microbes is their ability to gain resistance to antibiotics [1]. In
25 the recent years, antimicrobial peptides (AMPs) are investigated as attractive alternatives to conventional antibiotic
26 treatment. The acquisition of resistance to AMPs in microbes is much slower [3], moreover, they can be active against
27 pathogens that are resistant to antibiotics [4].

28 Typically, AMPs are amphiphatic; cationic amino acids build the hydrophylic face of the peptide, while hy-
29 drophobic residues dominate the opposite side of the molecule. Amphiphacity together with high charge allow AMPs
30 to invade and disrupt the negatively charged microbial cellular membrane [5]. Antimicrobial activity of peptides is
31 measured experimentally by determining its Minimal Inhibitory Concentration (MIC). The most prominent peptides
32 have low values of MIC, meaning that they remain active even in low concentrations, but their prevalence is limited.
33 Given the high therapeutic promise of AMPs, it is critical to design novel peptides that are nonexistent in nature and
34 could be synthesised and used to treat microbial infections in the clinic.

35 In biological labs, the process of identifying new antimicrobial peptides commonly proceeds by taking existing,
36 known AMPs as prototypes, and adding or substituting amino acids, aiming at increasing the resulting amphiphacity
37 and/or charge. Such generated peptides are subjected to synthesis attempt, and if synthesizable, their antimicrobial
38 activity is experimentally verified. First, this process is tedious, and time and cost consuming. Second, it is difficult
39 to improve existing AMPs, which already have good physicochemical properties. Finally, even if new candidates
40 are obtained in this way, the novel peptides will be similar in their sequence to existing peptides, and as such their
41 diversity is expected to be poor. Thus, there is a need to devise efficient and accurate *in silico* approaches to novel
42 AMP generation.

43 The problem of modelling AMPs was undertaken by a number of different computational approaches. One group
44 of these approaches are classifiers, which take a peptide as input and their task is to predict whether the peptide is an
45 AMP or not [6, 7, 8, 9], whether it is toxic [10, 11], or whether it is active [12, 13]. A related group of methods are
46 quantitative structure–activity relationship (QSAR) models [14, 15], which identify a set of structural features for a
47 given peptide, all of which are associated with the peptides being AMP, for example helical structure, amphipathicity,

48 etc. Next, the model is applied to a peptide database and peptides with the highest scores for features associated
49 with being AMP are chosen. As such, the QSAR methods can only score existing peptides and are not able to
50 directly generate new ones. Another approach is to use autoregressive models trained on AMP sequences for peptide
51 generation [16, 17, 18]. To generate new peptides, these models operate in an iterative manner. In each iteration, a
52 subsequence of the peptide constructed so far is given at input, and the model is used to propose the consecutive amino
53 acid in the sequence. Other approaches are based on the genetic algorithms [19, 20, 21, 12]. These methods iteratively
54 evolve a population of peptide sequences by adding random mutations, evaluating their fitness, and performing cross-
55 over and other evolutionary operations. Their performance depends on the choice of the method for introducing the
56 mutations and for evaluating their fitness. Finally, there are linguistic models [22], that consider peptides as a formal
57 language with grammar and vocabulary. By inserting alpha-helical patterns into AMP sequences in a sliding window
58 manner, they are able to generate novel sequences in few attempts.

59 Working in the peptide space (both amino acid sequence, as well as atomic composition, e.g. encoded with graph-
60 based representations such as the Simplified Molecular Input Line Entry Specification, or shortly SMILES [23]), as
61 it is the case of the QSAR, genetic algorithm-based methods, and linguistic approaches, has serious disadvantages.
62 First, the sequence space is sparse. Second, it is combinatorial and discrete, and thus highly dimensional, causing
63 these approaches to be computationally demanding and prone to quickly getting stuck in local minima [21]. On top
64 of that, similarity in this sequence space does not imply similarity of peptide function. Specifically, it is likely that
65 operations such as amino acid substitutions, deletions, or additions, making small changes to the sequence, have
66 large impact on amphiphacity or charge, and thus also antimicrobial activity of the peptide. Thus, it is desirable for
67 the computational approach to find a better, continuous, and reduced-dimensionality representation of peptides, and
68 operate on such representations instead.

69 Such representation learning approaches to peptide generation include GANs [24, 25] and variational autoen-
70 coders (VAE) [26, 13] as well as their conditional variants cGANs [27] and cVAEs [28, 29]. The conditional variants
71 enable generation of peptides satisfying a given condition. In contrast to VAE, training of GANs was reported to face
72 substantial technical obstacles, such as training instabilities and mode collapse [27].

73 On top of that, the existing approaches are not explicitly trained to perform all desired tasks. Specifically, almost
74 all of above generative models, except for the genetic algorithm and cVAEs, are suitable only for a generation mode,
75 which corresponds to random generation of AMPs, and which we refer to as *unconstrained* generation. In fact,

76 generation by improving existing peptides, which we call the *analogue generation*, should also be optimized during
77 training. Moreover, ideally, in the analogue generation, the peptides should be generable both from known active
78 AMP (positives) and non-AMPs (negatives). Indeed, the former mode would allow to directly mimic the experimental
79 approach, while the latter is expected to increase the diversity of the pool of generated peptides. To our knowledge,
80 none of the existing approaches are trained to improve non-AMPs. Finally, the results of the generative models
81 are rarely experimentally verified, and their functionality is usually not made available to non-technical users in a
82 digestible manner, e.g. as a web service.

83 Here, we propose HydrAMP, a novel approach for peptide generation, designed to address these needs. Hy-
84 drAMP is a cVAE-based model, which is specifically trained to perform analogue generation both from positives
85 and negatives, as well as for unconstrained generation. It learns a hidden space of meaningful peptide repres-
86 tations, which is disentangled from the set of antimicrobial conditions that a generated peptide is expected to sat-
87 isfy — whether it is supposed to be a highly active AMP or not. The model is available as a web-service at
88 www.hydramp.mimuw.edu.pl, and its results were experimentally verified and investigated in detail using *in*
89 *silico* molecular dynamics simulations. As such, HydrAMP is a step forward in the daunting task of generating novel,
90 highly active AMPs and fighting the problem of antimicrobial resistance.

91 2 Results

92 2.1 HydrAMP — a conditional, generative model of peptide sequences

93 HydrAMP is a model for generation of novel peptide sequences satisfying given antimicrobial activity conditions. A
94 pair of conditions, denoted $\mathbf{c} = (c_{AMP}, c_{MIC})$ specifies whether the generated peptide is supposed to be antimicrobial
95 (condition c_{AMP}) and whether it is supposed to have high antimicrobial activity, or, equivalently, low MIC (condition
96 c_{MIC}). Despite the fact that the feature of being AMP and being highly active are strongly related, we keep them as
97 separate conditions, because of existence of peptides that are known to be antimicrobial but have low activity.

98 The training data for HydrAMP consists of a curated data set of peptide sequences, including sequences that are
99 known to be AMP, sequences that are known to have a low MIC, and sequences collected from UniProt (Figure 1a).
100 The model is trained in three modes: *reconstruction*, *analogue* and *unconstrained* (Figure 1b). Training in the re-
101 construction mode facilitates the model to properly capture peptide sequences distribution, as well as those properties
102 that make them antimicrobial and active. This is achieved by ensuring that the reconstructed peptides are similar to

103 the input peptides from the training data and satisfy the same conditions. In the analogue mode, the model is trained
104 to generate analogues based on the provided prototype peptide and satisfying a specified condition. Finally, in the
105 unconstrained mode, the model is trained to generate peptides *de novo* that resemble training data and satisfy the
106 specified condition.

107 More formally, HydrAMP is an extension of a conditional variational autoencoder (cVAE). The model is opti-
108 mized to create a meaningful, latent, real-valued vector space representation of peptides, which is easier to sample
109 from and has a lower dimension than the original, highly dimensional and combinatorial space of peptide sequences.
110 Apart from standard neural network-based sub-models such as *Encoder* and *Decoder*, used in the cVAE framework
111 to operate on the latent representation in a probabilistic manner, the model utilizes also a *Classifier*. The Classifier is
112 also a neural network, which, unlike the Encoder and the Decoder, is pre-trained prior to HydrAMP training, and is
113 used in order to classify whether any given peptide is AMP or not, and whether it has a low MIC or not.

114 HydrAMP utilizes a number of regularization terms: latent reconstruction regularization, KL divergence, and
115 Jacobian disentanglement regularization (Figure 1b). The former two regularization terms are standard in the cVAE
116 framework. The latter is specifically introduced in this work for obtaining a disentanglement between the latent
117 representation of peptides and the condition. In this way, the latent space encodes the property of being a peptide,
118 while the condition independently encodes whether this peptide is supposed to be AMP or active (have low MIC).
119 See Methods for a detailed formal description of the model.

120 HydrAMP offers two generation modes: *analogue* and *unconstrained* (Figure 1c). The analogue mode improves
121 upon the common practice of novel peptide discovery followed in experimental labs. In contrast to the tedious trial and
122 error process of changing the original sequence, given the prototype and the desired condition, the model manipulates
123 the latent representation of the prototype instead. Given the favorable nature of the latent space, which spans real-
124 valued vectors that were trained as representations of valid peptides, and given that distances in the latent space
125 should reflect the dissimilarities between the peptides, the points in the latent space in close proximity to the point
126 representing the original peptide are good candidates for analogue samples. For such samples from the latent space,
127 the role of the Decoder is then to generate a sequence of amino acids satisfying the desired condition. HydrAMP
128 benefits from an additional temperature parameter τ that controls the creativity of analogue generation. Intuitively,
129 the temperature influences the radius with respect to the prototype point in the latent space within which the analogues
130 are searched for. Compared to the analogue mode, the unconstrained mode is more standard for cVAE and allows

131 generation of random peptides with either random, or desired condition. To this end, samples are generated from a
132 prior distribution over the latent space, and Decoder is used to produce sequences with the fixed condition.

133 **2.2 HydrAMP outperforms other models in the ability to generate antimicrobial and highly active peptide
134 candidates**

135 HydrAMP was compared to two alternative models: *Basic* and *PepCVAE* [28]. Basic is a standard cVAE, while PepC-
136 VAE is a state-of-the-art approach to peptide generation using the conditional variational autoencoder framework. In
137 case of Basic, only reconstruction mode training was performed. For PepCVAE we used reconstruction and uncon-
138 strained modes. Both models lack analogue generation and Jacobian disentanglement regularization (see Methods for
139 further details).

140 To evaluate the generation performance of the evaluated methods we inspected their creativity as the number
141 of generated peptides satisfying given conditions. We also inspected their ability to obtain desired antimicrobial
142 properties, as specified by setting the condition, in a number of different generation tasks. To this end, in each task,
143 each generated peptide p was assessed by the Classifier, and its probability of being AMP $\mathbb{P}_{M_{AMP}}(p)$ or being active
144 $\mathbb{P}_{M_{MIC}}(p)$ was recorded.

145 In order to assess the analogue generation mode, we first performed a series of experiments, in which HydrAMP
146 and the compared models were asked to generate analogues of known, existing AMPs (referred to as *positives*; see
147 Figure 2a). In these experiments, model was given a prototype sequence as input and the conditions were set to
148 $c_{AMP} = 1$ (being antimicrobial) and $c_{MIC} = 1$ (being highly active). A 1319 AMP peptides from the test set (not used
149 during training) were used as prototypes. We defined two distinct evaluation criteria: *discovery* and *improvement*,
150 with the former corresponding to the ability of simply generating analogues with good antimicrobial properties, and
151 the latter corresponding to generating analogues with properties strictly better than the input prototype. Specifically, a
152 peptide met the discovery criterion if it had a probability of being AMP greater than 0.8 and probability of having low
153 MIC greater than 0.5. A peptide met the improvement criterion if its probability of being AMP and the probability
154 of having low MIC were both greater than of the original peptide. Meeting the discovery criterion turned out to be a
155 relatively easy task, as novel analogues were accepted for nearly 50% of input positive prototypes for all models, with
156 HydrAMP showing a 4 percent point advantage in the fraction of accepted analogues (0.52) compared to the next best
157 model, Basic (0.48). In contrast, analogues that met the improvement criterion were produced only for a few percent

158 of prototypes. Here, based on the same set of prototype sequences, the HydrAMP model improved over twice (82) as
159 many peptides the PepCVAE (31) and over three times more than the Basic model (23). These results show that the
160 HydrAMP model is more creative than the compared models and has the capabilities of introducing new analogues
161 for original prototypes.

162 For further analysis of the analogue generation, we gave HydrAMP and the compared models a harder task of
163 generating analogues for 1253 known non-AMP peptides (negatives) from the test set (Figure 2b). Unsurprisingly,
164 meeting the discovery criterion was more challenging where the negatives were given as input compared to the pos-
165 itives. Still, HydrAMP managed to discover analogues for 82 prototypes, which is over 60% more than PepCVAE
166 (52) and Basic (51) models. Notably, HydrAMP was also able to improve over 50% of the test set negatives, three
167 times more than the best of the competing models, PepCVAE. In order to compare the antimicrobial properties of the
168 prototype negatives and their analogues that met the discovery criterion, we analyzed the probability of being AMP
169 and being active of both prototypes and the analogues.

170 We also compared these probability distributions against the distributions for all peptides from the test data.
171 HydrAMP was able to produce analogues that met discovery criterion for peptides that had lower *a priori* probability
172 of being AMP (Figure 2c) and lower probability of being highly active (Figure 2d) than its competitors.

173 In contrast, Basic and PepCVAE models produced analogues that met the discovery criterion for peptides that were
174 already initially likely to be antimicrobial and active. The outstanding performance of HydrAMP in generating highly
175 antimicrobial and active novel peptides based on experimentally-validated non-AMP prototypes shows its potential
176 to provide truly novel antimicrobial peptides and increase the diversity of the pool of AMP sequences. Indeed, in
177 contrast to analogues produced from positive prototypes, those peptides are expected to have sequences that largely
178 differ from the sequences of known AMPs.

179 In order to assess the creativity of HydrAMP model in the analogue generation, we evaluated the number of
180 different analogues created using two popular AMP peptides as prototypes: Pexiganan and CAMEL (Figure 2ef).
181 Here, we used an additional parameter of HydrAMP analogue generation — the temperature $\tau > 0$, which controls
182 the level of peptide alternations with respect to the original peptide (Figure 1c). Indeed, the greater the temperature,
183 the more the generated analogues differ from the prototype (Figure 2ef). The ability to control the creativity of the
184 model is important. The more similar a newly created analogue is to the prototype one, the more likely it is to preserve
185 the physicochemical properties of the original peptide. On the other hand, the more alternations introduced, the larger

186 the number of generated novel peptides.

187 We assessed the unconstrained generation abilities of HydrAMP in comparison to other methods by generation
188 of peptides at random in two modes: *positive* and *negative*. In the case of the *positive* mode we randomly sampled
189 the latent representation variable and set the condition of the new peptide p to have a high probability of being AMP
190 ($\mathbb{P}_{M_{AMP}}(p)$) and a high probability of being active ($\mathbb{P}_{M_{MIC}}(p)$). In the negative mode, we set the peptide conditions
191 to be non-AMP ($c_{AMP} = 0$) and not active ($c_{MIC} = 0$). Peptides generated by HydrAMP were more likely to follow
192 the desired conditions than the competing models both for AMP (Figure 2g) and MIC (Figure 2h) conditions. The
193 advantage of HydrAMP was the most noticeable in the case of the probability of being AMP: the median probability
194 of being AMP for peptides generated by HydrAMP was around 1, while for the next best model, PepCVAE, it was
195 around 0.5 (Figure 2g).

196 In order to confirm that HydrAMP is able to suggest new, synthesizable active AMP peptides when using the un-
197 constrained mode we tested to what degree peptides generated in this mode match appropriate criteria (Figure 2i). For
198 that, we generated 50k candidate peptides and run four experiments confirming their properties. First, we computed
199 the fraction of such peptides p which had high probability of being AMP ($\mathbb{P}_{M_{AMP}} > 0.8$) and high probability of being
200 active ($\mathbb{P}_{M_{MIC}}(p) > 0.5$). Next, we assumed their secondary structure as alpha-helical and tested their amphipathicity
201 using hydrophobic moment [30]. Peptides with amphiphatic alpha-helical structure are known to be easily synthesiz-
202 able and their mode of action has been thoroughly studied [31]. Accordingly, we computed the fraction of peptides
203 with the hydrophobic moment > 0.4 (the mean hydrophobic moment of the positive peptides no longer than 26 amino
204 acids). Finally, we evaluated the fraction of peptides that had charge > 4 (the mean charge of the positive peptides no
205 longer than 26 amino acids; see Supplementary Figure S1 for details of the hydrophobic moment and charge thresh-
206 olds selection). HydrAMP suggested the largest number of peptides that were confirmed as positives, were sufficiently
207 amphipathic, and were positively charged, in each condition separately. Eventually, HydrAMP created almost 50%
208 more peptide candidates that matched all three conditions than its best competitor (Basic).

209 **2.3 HydrAMP generates peptides with desired physicochemical properties**

210 Next, we evaluated HydrAMP by inspecting the physicochemical properties of peptides that it generates, in compar-
211 ison to the properties of known peptides as well as peptides generated by PepCVAE and Basic (Figure 3). Physico-
212 chemical properties of antimicrobial (positive) peptides differ from peptides that were experimentally verified not to

213 be antimicrobial (negative peptides). Indeed, a comparison of the distributions indicated that isoelectric point (Figure
214 3a), charge (Figure 3d), hydrophobic moment (Figure 3g), and aromaticity (Figure 3j) are significantly larger
215 (one-sided Mann-Whitney test p-value < 0.05) for known positives than for negatives.

216 We first inspected the performance of HydrAMP and other approaches in the task of finding positive peptides based
217 on negative prototypes in the analogue generation. Given such significant differences between negatives and positives,
218 this requires the introduction of a shift in the physicochemical properties from the non-AMP prototypes to the newly
219 generated peptides. In this task, HydrAMP showed a capacity to generate analogues with the desired significant
220 increase (one-sided Wilcoxon test p-value < 0.05) of all investigated properties: isoelectric point (Figure 3b), charge
221 (Figure 3e), hydrophobic moment (Figure 3h), and aromaticity (Figure 3k). We tested three temperature parameter
222 setups: a conservative $\tau = 1.0$, and more explorative $\tau = 2.0$ and $\tau = 5.0$ levels. For higher temperature levels, the level
223 of improvement was much higher than for Basic and PepCVAE models. This implies that we can control the balance
224 between physicochemical improvement and the degree of changes between new analogues and their prototypes. We
225 confirmed that these results could not be obtained by chance by computing physicochemical properties of a randomly
226 sampled subset of the UniProt dataset and peptides for which we randomly sampled a sequence of amino acids. In
227 both of these cases, HydrAMP in explorative temperature setups produces peptides with better qualities. In contrast
228 to HydrAMP, all four physicochemical properties of peptides generated by PepCVAE or Basic showed no significant
229 difference to the properties of known negatives.

230 Second, we evaluated HydrAMP and other approaches in a task of improving the positives. Here the challenge
231 is different than in the previous task, as it is hard to improve peptides that are already "good" (are already AMP and
232 active). Here, for all analyzed physicochemical properties, HydrAMP generated peptides with significantly better
233 (one-sided Wilcoxon test p-value < 0.05) properties than the input positive prototypes (Figure 3c,f,i,l). The benefit
234 of the model's creativity using a larger temperature parameter is most visible for aromaticity (Figure 3l). PepCVAE
235 and Basic performed only slightly worse in this task, either producing peptides that did not improve the hydrophobic
236 moment (PepCVAE; Figure 3i) or aromaticity (Basic; Figure 3l).

237 Finally, we evaluated the physicochemical properties of positive and negative peptides generated by HydrAMP in
238 the unconstrained mode, in comparison to peptides generated by other methods (Supplementary Figure S2). For all
239 four analyzed physicochemical properties, there was large and significant difference between their distributions for
240 HydrAMP generated negatives and positives (one-sided Wilcoxon test p-value < 0.05). For PepCVAE and Basic, the

241 differences between negatives and positives were also significant, but the medians of the distributions did not differ
242 by as large amount as for HydrAMP. We confirmed that the amino acid distribution of the peptides generated in the
243 unconstrained mode is in agreement with the true amino acid frequencies (Supplementary Figure S3). High content
244 of lysine (K) and arginine (R), as well as low content of negatively charged glutamic acid (E) and aspartic acid (D)
245 contribute to the positive net charge.

246 Overall, these results illustrate the superior performance of HydrAMP in generating peptides with desired physico-
247 chemical properties, reflecting the properties observed for real peptides.

248 **2.4 HydrAMP suggested valid novel peptides**

249 Finally, we inspected the ability of HydrAMP to generate novel peptides using experimental wet lab validation (for
250 details see Supplementary Material S5). To this end, we applied HydrAMP in the analogue mode, with temperature
251 (creativity) parameter $\tau = 1.0$, treating Pexiganan and Temporin-A as prototypes. The low creativity parameter choice
252 was justified by the fact that we intended to obtain novel peptides that were similar to the prototypes. For each
253 prototype, we first generated a set of 900 positive analogues. Next, we applied stringent filtering criteria to both
254 generated sets of peptides (see Biological filtering criteria) to increase the chance of peptides being synthesizable and
255 were left with 92 sequences for Pexiganan and 84 for Temporin-A. Out of these candidates, five positive analogues
256 of Pexiganan and five of Temporin-A were selected for experimental validation. One of the selected Pexiganan
257 analogues did not synthesize. The remaining were investigated experimentally and their antimicrobial activity was
258 tested against two *E. coli* strains (Table 1; Methods). Laboratory experiments validated the known and predicted by
259 the Classifier very high antimicrobial activity of Pexiganan. Out of four synthesizable analogues of Pexiganan, one
260 showed even higher activity than that of Pexiganan ($MIC = 2 \mu\text{g/mL}$). This novel validated antimicrobial peptide was
261 called Hydraganan. Another predicted analogue was confirmed as AMP and of high activity ($MIC = 16 \mu\text{g/mL}$).

262 The Classifier model predicted high probability of being antimicrobial, and a very low probability of being highly
263 active for Temporin-A. The low activity was confirmed in the lab ($MIC = 256 \mu\text{g/mL}$). All five predicted positive
264 analogues of Temporin-A also showed low antimicrobial activity ($MIC \geq 512 \mu\text{g/mL}$). As controls, we randomly
265 selected and validated two peptides generated as negative analogues by HydrAMP, one for Pexiganan, and one for
266 Temporin-A. Both the negative analogues were validated as inactive ($MIC > 512 \mu\text{g/mL}$).

267 **2.5 Simulations confirmed that Hydraganan penetrates the cell membrane**

268 To better understand the functional properties of Hydraganan and of the experimentally validated negative analogue of
269 Pexiganan, we performed extensive, fully atomistic simulations of their behavior in the presence of a lipid membrane
270 (Figure 4a, b). Each peptide was constructed as a regular α -helical structure and placed in aqueous compartment
271 of the simulation box with its helical axis parallel to the membrane plane, at three different orientations. During the
272 simulations we monitored the stability of peptides α -helical structure as well as the degree of their association with the
273 membrane. The latter was assessed based on consecutive, 25 ns long simulation blocks, by considering a parameter
274 $S \in [0, 1]$ that indicates the fraction of peptide heavy atoms distribution along the membrane normal, that penetrates
275 towards the bilayer core below a dividing plane corresponding to a depth at which the distribution of membrane
276 heavy atoms reaches half of its maximum value (Figure 4c). Accordingly, $S = 0$ indicates no association, while $S = 1$
277 represents full peptide burial.

278 In the case of Hydraganan, irrespective of initial orientation, we observed peptide association with the membrane
279 within the first 250 ns of the simulation time, as indicated by S values increasing above 0.5 (Figure 4d, lower plot).
280 In all cases the association was followed by complete peptide burial ($S \rightarrow 1$) within 500 ns. In contrast, the negative
281 Pexiganan analogue only loosely adhered to lipid bilayer surface and revealed no tendency to penetrate into its core,
282 with S values remaining around 0.25 till the end of simulations. Notably, the active peptide consistently maintained
283 ~ 0.75 fraction of helical geometry, that is considerably more than the inactive one, whose helical structure content
284 dropped well below 0.5 already within the first 200 ns (Figure 4d, upper plot).

285 Together these findings underscore the importance of a stable α -helical scaffold which is necessary to secure
286 properly aligned hydrophobic surface patch on one peptide side and oppositely facing cluster of hydrophilic or charged
287 side chains. While the former provides a driving force for peptide insertion into the nonpolar membrane core, the latter
288 apparently prevents membrane defect from closing. Notably, these features rely not merely on individual amino acids
289 but rather on their appropriate distribution within the sequence that warrants correct placement upon folding as well
290 as helical propensity of the resulting structure.

291 **3 Discussion**

292 In this work we have proposed HydrAMP, a generative model for antimicrobial peptides discovery. It leverages
293 a conditional variational autoencoder to offer two functionalities: generating analogues of existing peptides with

improved antimicrobial properties (analogue generation) and generating peptides *de novo* (unconstrained generation). This is enabled by a continuous peptide representation of reduced dimensionality with disentangled antimicrobial conditions c_{AMP}, c_{MIC} . Additionally, this representation is directly optimized to not only properly represent the known peptides but also to efficiently generate new candidates.

We have evaluated the model’s ability to improve existing antimicrobial peptides by producing analogues of Pexiganan and Temporin-A. We obtained Hydraganan, a potent antimicrobial peptide displaying better activity than Pexiganan, and another Pexiganan analogue of high activity. Hydraganan was verified experimentally and by molecular dynamics simulations. Importantly, the simulations were performed in the presence of a lipid membrane. To facilitate the usage of HydrAMP model, we developed a web service available freely at <https://hydramp.mimuw.edu.pl/>.

HydrAMP bears several novelties and advantages in comparison to existing approaches. First, in contrast to previous VAE/WAE-based approaches [26, 28, 29], HydrAMP was trained specifically for the task of analogue generation. Additionally, HydrAMP is the first model trained and used to identify active analogues of non-AMP prototypes. Third, leveraging a Gumbel-Softmax approximation [32] enabled a continuous approximation of sampling in the discrete space of amino acid sequences and thus a direct optimization of peptides generated by the model. Before, such optimizations required a complex multi-stage training [28]. Finally, HydrAMP is the only model controls in a parametrized way the model creativity understood as the number of modifications introduced to the query peptide.

Although HydrAMP conveys advancement over previous approaches, it still could be extended in several ways. First, HydrAMP could be enriched with a popular attention mechanism [33]. The architecture of the model allows easy replacement of both the Encoder and the Decoder with transformer modules [33]. It is not clear, however, that such an extension of the model would improve its performance, as initial evidence suggested that attention-based models might work worse for peptide modelling than recurrent models [34]. Additionally, we considered amino acid sequence only. Instead, we could leverage structure prediction models such as AlphaFold [35], and extend HydrAMP training procedure to directly optimize alpha-helix propensity and other structural features of AMPs. In this work, the loss term responsible for reconstruction objective treats each of the amino acids in the sequence as independent. However, the probability of each amino acid being present is dependent on proceeding and following amino acids. The local context can also affect the antimicrobial activity of a given peptide, as shown in [36].

Finally, the applicability of the model could be also extended. HydrAMP does not consider the host toxicity of

322 the peptides. Successfully optimizing both activity and host toxicity within the same model would provide a powerful
323 tool for AMP design. Addressing the toxicity is an urgent matter as only highly selective peptides can be used in
324 treatment of human subjects. Additionally, we trained the model to target only *E. coli* strains. Depending on the data
325 availability, it could be retrained to target other strains, either Gram-positive or multi-drug resistant strains.

326 Antimicrobial resistance problem remains a serious threat that needs dire actions. HydrAMP is a novel, powerful
327 tool capable of suggesting new antimicrobial peptides what has been shown both through wet-lab evaluation and
328 molecular dynamics simulations. Thus, by quick indication of possible candidates HydrAMPs is making progress
329 towards creation of a new generation of antibiotics.

330 **4 Methods**

331 **4.1 Data collection**

332 The training data for the model is a curated data set of a total of 247 506 peptide sequences collected from three
333 sources: MIC data collected by [12], AMP data from known AMP databases, and UniProt data [37]). To speed up
334 the training process and control the synthesis costs, all selected training sequences have length of at most 25 amino
335 acids and contain only standard amino acids. Sequences shorter than 25 amino acids were padded using additional
336 padding character.

337 **MIC data** The MIC data set consists of peptides with experimentally proven antimicrobial activity and measured
338 MIC values downloaded from GRAMPA database [12]. Of 8049 entries only 4546 of them are unique sequences. We
339 select those peptides which were experimentally tested for activity against *E. coli* strains. MIC values for peptides
340 with multiple measurements are averaged resulting in 4546 entries. Only 3444 peptides have the required length of
341 25 amino acids. Peptides with $\text{MIC} < 30 \mu\text{g/ml}$ are labeled as active (positive), while peptides with $\text{MIC} \geq 30 \mu\text{g/ml}$
342 are labelled as inactive (negative). MIC data set contains 2126 positives and 1318 negatives.

343 **AMP data** The AMP data consists of positive and negative data set. Positive examples are sequences from manually
344 curated AMP databases. We combine experimentally validated peptides from dbAMP [38], AMP Scanner [8], and
345 DRAMP [39] databases. Duplicate sequences are removed. Negative examples are assumed to be biologically inactive
346 and are obtained manually using UniProt search filters, requiring subcellular location: cytoplasm, and excluding the
347 following properties: antimicrobial, antibiotic, antiviral, antifungal, effector, excreted. To increase data set diversity,

348 negative sequences sharing $\geq 40\%$ sequence identity are removed, and replaced with the representative sequences
349 of the clusters using CD-HIT [40, 41]. The resulting set of representative sequences contains only sequence that
350 are longer than 25 amino acids, thus negative sequences are randomly cropped to match the positive data set length
351 distribution in order to avoid length bias. The positive and negative data sets are of equal size of 11,131 sequences
352 each.

353 ***UniProt* data** To extend the biological diversity in the training process we downloaded sequences of unknown
354 antimicrobial properties of the desired length from UniProt database. This gave 225 244 additional sequences with no
355 duplicates.

356 **4.2 AMP and MIC classifiers learning**

357 In order to predict the properties of generated peptides, we trained a pair of classifiers, that for a given peptide p ,
358 predict its probabilities of being antimicrobial and active. For the prediction of a given peptide being antimicrobial
359 (AMP), we implemented and trained the model from AMP Scanner [8], using AMP data. We refer to this model
360 as M_{AMP} . For the prediction of peptide activity, we trained a model using MIC data, denoted M_{MIC} , with a custom
361 architecture. The model consists of six layers. The first layer is an one-hot encoded input in form of a sequence of
362 amino acids. The second layer is an 128-dimensional embedding layer of each of the amino acids. Next, we use the
363 LSTM layer of 64 units [42]. Downsampling is performed by 1-dimensional pooling with kernel size of 5 and stride
364 of 5. Another LSTM layer of 100 units is used where only the last output is return. The final output is fully connected
365 layer with a sigmoid activation.

366 For a given peptide p , the M_{AMP} returns the probability of p being antimicrobial, denoted $\mathbb{P}_{M_{AMP}}(p)$. The M_{MIC}
367 returns the probability of p being active, denoted $\mathbb{P}_{M_{MIC}}(p)$. From now on we assume that these probabilities are ob-
368 tained only using M_{AMP} and M_{MIC} classifiers, and we refer to them jointly as Classifier. Both models are implemented
369 in Keras [43].

370 Cross-validation results indicate highly accurate classification results for both M_{AMP} and M_{MIC} (Supplementary
371 Table S1).

372 **4.3 HydrAMP model**

373 HydrAMP is an extended conditional VAE (cVAE) model. Its main generative part is a Decoder model that given a
374 *latent variable* $z \in \mathbb{R}^{latent}$ and a pair of conditions $\mathbf{c} = (c_{AMP}, c_{MIC})$ produces a distribution over peptides $Dec(z, \mathbf{c})$.
375 We refer to the likelihood of a peptide p w.r.t. to this distribution as $\mathbb{P}_{Dec(z, \mathbf{c})}(p)$. The latent variable is assumed to
376 follow the *latent prior* distribution $P_z \sim \mathcal{N}(0, I)$.

377 The Decoder is trained so that the peptides sampled from $Dec(z, \mathbf{c})$ follow a given pair of conditions \mathbf{c} and re-
378 semble valid peptides from the training dataset. As optimizing the Decoder directly is not feasible, we introduced an
379 additional Encoder model trained to provide a variational approximation $q(z|p)$ of the posterior distribution $\mathbb{P}(z|p)$.
380 The variational posterior approximation for a peptide p is set to be a normal distribution $\mathcal{N}(\mu_{q(\cdot|p)}, diag(\sigma_{q(\cdot|p)}))$,
381 where $\mu_{q(\cdot|p)} \in \mathbb{R}^{latent}$ and $\sigma_{q(\cdot|p)} \in \mathbb{R}_+^{latent}$. Both the Decoder and Encoder are modeled as neural networks. For the
382 detailed architecture see Supplementary Material S3.

383 The HydrAMP model is optimized using three objectives: reconstruction, analogue (see Supplementary Mate-
384 rial S1.1), and unconstrained (see Supplementary Material S1.2). The reconstruction objective aims at teaching the
385 Decoder how to generate valid peptide structures by reconstructing known peptides. The analogue and unconstrained
386 objectives mimic the process of the analogue and unconstrained generation during training. Besides that, we also
387 applied a two-fold regularization to the HydrAMP model: the Jacobian disentanglement regularization to encourage
388 disentanglement between latent variable z and a pair of conditions \mathbf{c} , and latent reconstruction regularization for better
389 latent variable preservation properties.

388 In the formulas below we use the following notation. Denote a constant $c \in [0, 1]$, p a peptide and $P_M(p)$ its
389 probability in a classifier model M , with $M \in \{M_{AMP}, M_{MIC}\}$. Let

$$H_M(c, p) = \log (\mathbb{P}_M(p)^c (1 - \mathbb{P}_M(p))^{1-c}), \quad (1)$$

be the cross-entropy between the $Bernoulli(c)$ and $Bernoulli(\mathbb{P}_M(p))$. We define

$$H_\Sigma(\mathbf{c} = (c_{AMP}, c_{MIC}), p) = \sum_{cond \in \{AMP, MIC\}} H_{M_{cond}}(c_{cond}, p), \quad (2)$$

390 where $\mathbf{c} = (c_{AMP}, c_{MIC})$ is the pair of conditions, as the sum of the cross entropies for the two different conditions
391 c_{AMP}, c_{MIC} and their probabilities $\mathbb{P}_{M_{MIC}}(p)$ and $\mathbb{P}_{M_{AMP}}(p)$, respectively.

392 **4.3.1 Reconstruction objective**

393 The reconstruction objective forces the model to capture the structure of valid peptides collected from available
 394 databases. We achieve this by training the Decoder and Encoder maximizing the conditional evidence lower bound
 395 (ELBO) introduced in [44]. For each peptide $p \sim \mathbb{P}_X$, we compute its pair of conditions $\mathbf{c}_p = (\mathbb{P}_{AMP}(p), \mathbb{P}_{MIC}(p))$
 396 using the Classifier. Next, we maximize a conditional ELBO given by:

$$ELBO_{rec}^{\beta} = \mathbb{E}_{z \sim q(z|p)} (\log \mathbb{P}_{Dec(z, \mathbf{c}_p)}(p) + \quad (3)$$

$$\lambda_{rec}^{class} \mathbb{E}_{p' \sim Dec(z, \mathbf{c}_p)} H_{\Sigma}(\mathbf{c}_p, p') \quad (4)$$

$$\beta \cdot KL(q(z|p) \| P_z), \quad (5)$$

397 where (3) is the expected log likelihood of reconstruction of the initial peptide p , (4) is the expected log likelihood
 398 of recovering the initial peptide pair of conditions \mathbf{c}_p with parameter $\lambda_{rec}^{class} > 0$ and (5) is a β -VAE regularization
 399 term [45] with parameter $\beta > 0$ decaying in the process of training. Parameters β and λ_{rec}^{class} control the trade-off
 400 between reconstruction of the original peptide, satisfying the peptide condition and keeping the posterior approxima-
 401 tion $q(z|p)$ close to the prior. The expectations w.r.t. $q(z|p)$ are obtained using a reparametrization trick [46] and are
 402 approximated using a single sample from $q(z|p)$.

403 **4.3.2 Jacobian disentanglement regularization**

404 For every generation process used by the HydrAMP model, a newly generated peptide should have properties
 405 provided by a pair of conditions \mathbf{c} . To measure that, let us define an average condition reconstruction function of the
 406 Dec distribution as:

$$ACR^{Dec}(z, c = (c_{AMP}, c_{MIC})) = \mathbb{E}_{p \sim Dec(z, c_{AMP})} (\mathbb{P}_{AMP}(p), \mathbb{P}_{MIC}(p)). \quad (6)$$

407 ACR^{Dec} measures the expected likelihood of the peptides sampled from the distribution Dec modeled by the Decoder,
 408 for a given z and pair of conditions \mathbf{c} , actually satisfying \mathbf{c} . Ideally $ACR^{Dec}(z, \mathbf{c}) = \mathbf{c}$, which means that on average
 409 peptides sampled from $Dec(z, \mathbf{c})$ have properties defined by the pair of conditions \mathbf{c} . This means that in an ideal
 410 scenario the ACR^{Dec} is constant w.r.t. z and in case when ACR^{Dec} is differentiable w.r.t. to z , the following condition

411 holds:

$$\frac{\partial ACR^{Dec}}{\partial z} \equiv \mathbf{0}, \quad (7)$$

412 where $\mathbf{0}$ is an all zero matrix. In that case z and \mathbf{c} are disentangled w.r.t. to ACR^{Dec} , because any change of z does not
413 affect the expected pair of conditions of newly generated candidates. In order to impose this property we introduce
414 the following Jacobian disentanglement regularization function:

$$JDR^{Dec}(z, \mathbf{c}) = \sum_{i=1, j=1}^{2, latent} Huber\left(\frac{\partial ACR_i^{Dec}(z, \mathbf{c})}{\partial z_j}\right), \quad (8)$$

415 where $Huber : \mathbb{R} \rightarrow \mathbb{R}$ (sometimes also referred as a smooth L1) is given by

$$Huber(x) = \min(|x|, x^2). \quad (9)$$

416 We use the Huber function as it is less prone to be affected by outlier examples.

417 Accordingly, we extended reconstruction objective with the following term:

$$JDR_{rec} = \mathbb{E}_{z \sim q(z|p)} JDR^{Dec}(z, \mathbf{c}_p), \quad (10)$$

418 where p is a peptide being reconstructed and \mathbf{c}_p is its pair of conditions. We approximate this expectation with a single
419 sample from $q(z|p)$ using the reparametrization trick.

420 Analogue and unconstrained objectives were also extended with the Jacobian disentanglement regularization term.

421 See Supplementary Material S2.1 for the details.

422 4.3.3 Latent reconstruction regularization

423 In the cVAE framework, the Decoder plays a role similar to the inverse function of the Encoder. Indeed, the
424 Decoder aims to reconstruct the peptide fed to the Encoder that is sampled from a posterior distribution generated
425 by the Encoder. To further impose that relation, similarly to [28], we introduced an additional latent reconstruction
426 regularization objective. Consider a peptide p and its posterior mean $\mu_{q(z|p)}$ given by the Encoder. Peptide p' returned
427 by the Decoder for a point sampled from that posterior can be given as input to the Encoder and will obtain its posterior
428 mean $\mu_{q(z|p')}$. The latent reconstruction regularization objective enforces the two posterior means to be similar. To

429 this end, we minimize the following expectation for the reconstruction objective:

$$LRR_{rec} = \mathbb{E}_{z \sim q(z|p)} \mathbb{E}_{p' \sim Dec(z, \mathbf{c}_p)} \|\mu_{q(\cdot|p)} - \mu_{q(\cdot|p')}\|_2^2, \quad (11)$$

430 where p is a reconstructed peptide and \mathbf{c}_p is its pair of conditions. Using a reparametrization trick, we approximate
431 this expectation with a single sample from $q(z|p)$ and the expectation w.r.t. Dec is approximated using a Gumbel
432 Softmax [32].

433 When the expectation above is low, the Encoder preserves the latent code of the average peptide sampled from the
434 Decoder. This property is essential especially for the analogue generation, as we assume the similarity between the
435 analogue and original prototype because we sample both from precisely the single posterior distribution over latent
436 codes. If the Encoder preserves the latent code of a generated analogue, then its similarity to prototype is granted for
437 continuous Decoder models.

438 Analogue and unconstrained objectives were also extended with the latent reconstruction regularization terms.
439 See Supplementary Material S2.2 for the details.

440 4.4 Basic and PepCVAE models

441 We compared HydrAMP with two other models: *Basic* and *PepCVAE* [28]. We used our own implementation of the
442 PepCVAE model, as its code was not made publicly available by the authors.

443 *Basic* model corresponds to the standard cVAE model (see [44]), and is trained in the same manner as HydrAMP,
444 but is optimized only for reconstruction objective and uses only the latent reconstruction regularization. PepCVAE
445 model was trained to optimize the same objectives as Basic, but was additionally optimized for the unconstrained
446 objective. Both PepCVAE and Basic models lack optimization of analogue objective and Jacobian disentanglement
447 regularization, which are incorporated in HydrAMP.

448 Since the Basic, PepCVAE and HydrAMP are increasingly complex, such a selection of models for comparison
449 effectively implements an ablation study.

450 4.4.1 Training procedure

451 We trained all models (HydrAMP, Basic, and PepCVAE) using ADAM [47] optimizer. The batch size was equal
452 to 384, and each batch consisted of 128 peptides from AMP, 128 from MIC data, and 128 from UniProt data. We
453 trained every model for 40 epochs. Reconstruction and analogue objectives were optimized using all peptides in each

454 batch. Additionally, in each iteration, the unconstrained objective was optimized using 128 samples from P_z . The
455 Gumbel temperature used in Gumbel Softmax [32], t , was scheduled using exponential decay from 2.0 to 0.1 for 24
456 epochs and then kept stable at 0.1. The β parameter was increased from 10^{-4} to 10^{-2} via exponential annealing.

457 For the loss function, evaluation metrics and model selection details for training of HydrAMP, Basic and PepCVAE
458 models see Supplementary Material S4.

459 **4.5 Post-training prior refinement**

Following successful results presented in [48], after the end of the training, we refined our P_z prior distribution to better match an aggregated posterior:

$$\mathbb{P}_z^{agg} = \mathbb{E}_{p \in \mathcal{X}} q(\cdot | p), \quad (12)$$

460 which is an average of all posterior distributions of peptides from dataset \mathcal{X} . According to [49] this distribution is
461 the latent prior distribution which maximizes likelihood of data from \mathcal{X} when Encoder and Decoder models are fixed.
462 However, this property makes it prone to over-fitting. Because of that we decided to use less complicated distribution
463 to approximate the aggregated posterior. This new distribution $\hat{\mathbb{P}}_z^{agg}$ is set to be a normal distribution $\hat{\mathbb{P}}_z^{agg} = \mathcal{N}(\hat{\mu}, \hat{\Sigma})$
464 optimized to maximize likelihood of the set of aggregated variational posterior means $\{\mu_{q(\cdot|p)} | p \in \mathcal{X}\}$. The distribu-
465 tion parameters $\hat{\mu}, \hat{\Sigma}$ are selected using a classical PCA algorithm [50].

466 **4.6 Generation modes of peptides**

467 After the model is trained we use it in order to generate novel peptides. There are the following modes of this process:

468 **4.6.1 Unconstrained generation**

469 The following algorithm is used for generation of active and antimicrobial peptides in an unconstrained manner
470 where z is sampled from a refined prior $\hat{\mathbb{P}}_z^{agg}$:

471 The algorithm above refers to the positive mode, while in the negative mode we sample peptides with conditions
472 ($c^{AMP} = 0, c^{MIC} = 0$). We skip peptides with $\mathbb{P}_{M_{AMP}}(p) > 0.2$ and select the peptide with the lowest $\mathbb{P}_{M_{MIC}}(p)$.

473 **4.6.2 Analogue generation**

474 The following algorithm was used for generation of active peptides similar to prototype peptide p_{proto} . In this

Data: A number of tries for generation `nb_of_tries`.
Result: A new active and anti-microbial peptide sampled from $\hat{\mathbb{P}}_z^{agg}$.

```

 $z \leftarrow sample(\hat{\mathbb{P}}_z^{agg});$ 
 $best\_candidate \leftarrow None;$ 
 $best\_candidate\_mic \leftarrow 0;$ 
for  $i \leftarrow range(nb\_of\_tries)$  do
     $new\_candidate \leftarrow sample(Dec(z, (c^{AMP} = 1, c^{MIC} = 1)));$ 
    if  $\mathbb{P}_{M_{AMP}}(new\_candidate) > 0.8$  and  $\mathbb{P}_{M_{MIC}}(new\_candidate) > best\_candidate\_mic$  then
         $best\_candidate \leftarrow new\_candidate;$ 
         $best\_candidate\_mic \leftarrow \mathbb{P}_{M_{MIC}}(new\_candidate);$ 
    end
end
return  $best\_candidate;$ 
```

Algorithm 1: Unconstrained generation in a positive mode

475 algorithm we introduce a creativity parameter $\tau \in (0, +\infty)$. Prototypes are sampled from a modified variational
476 posterior $\mathcal{N}(\mu_{q(\cdot|p_{proto})}, \tau^2 \cdot \sigma_{q(\cdot|p_{proto})})$ with a covariance matrix rescaled by a factor of τ^2 . This means that the closer
477 τ is to 0 - the peptide sampled is similar to the one assigned to the posterior mode. On the other hand - for $\tau > 1$ the
478 sampling probability distribution has the same mean but greater variance than in case of posterior approximation what
479 encourages generating peptides differing from p_{proto} to a greater degree.

Data: A prototype peptide p_{proto} , creativity parameter $\tau \in (0, +\infty)$, number of tries for generation
`nb_of_tries`.
Result: A new active and anti-microbial peptide sampled from similar to peptide p_{proto} .

```

 $\mu_{q(\cdot|p_{proto})}, \sigma_{q(\cdot|p_{proto})} \leftarrow Enc(p_{proto});$ 
 $best\_candidate \leftarrow None;$ 
 $best\_candidate\_mic \leftarrow 0;$ 
for  $i$  in  $range(nb\_of\_tries)$  do
     $z_{proto} \sim \mathcal{N}(\mu_{q(\cdot|p_{proto})}, \tau^2 \cdot \sigma_{q(\cdot|p_{proto})});$ 
     $new\_candidate \sim Dec(z_{proto}, (c^{AMP} = 1, c^{MIC} = 1));$ 
    if  $\mathbb{P}_{M_{AMP}}(new\_candidate) \geq 0.8$  and  $\mathbb{P}_{M_{MIC}}(new\_candidate) > best\_candidate\_mic$  then
         $best\_candidate \leftarrow new\_candidate;$ 
         $best\_candidate\_mic \leftarrow \mathbb{P}_{M_{MIC}}(new\_candidate);$ 
    end
end
return  $best\_candidate;$ 
```

Algorithm 2: Analogue generation for a positive mode

480 An analogue meets the improvement criteria when it increased $\mathbb{P}_{M_{AMP}}(p)$ and $\mathbb{P}_{M_{MIC}}(p)$ with respect to the input
481 peptide. An analogue meets the discovery criteria with $\mathbb{P}_{M_{AMP}}(p) \geq 0.8$ and $\mathbb{P}_{M_{MIC}}(p) > 0.5$.

482 **4.7 Biological filtering criteria**

483

484 In general, the biological criteria serve as approximation of expert selection that takes into account peptide synthe-
485 sizability. First, we filter out all of the known AMPs we collected in our AMP data set. Then, we exclude sequences
486 in which in a window of 5 amino acids there were more than 3 positively charged amino acids (K, R). Finally, we
487 remove sequences in which occur three hydrophobic amino acids in a row. We consider as hydrophobic following
488 amino acids based on Eisenberg scale [51]: F, I, L, V, W, M, A.

489 In case of selection of peptides for experimental validation we use more stringent criteria. We remove sequences
490 of known AMPs, and sequences with accumulation of positive charge, as described above. Additionally, we remove
491 any sequence in which three amino acids in a row are the same. We also exclude sequences containing cysteines (C).

492 **4.8 Computer simulations of peptide-membrane systems**

493 Given the amino acids sequence of interest, a peptide starting structure was modelled as a regular α -helix using
494 the Discovery Studio Visualizer 2021 program (Dassault Systèmes, BIOVIA) [52]. It was then submitted to the
495 CHARMM-GUI service [53] for peptide-membrane system construction. Standard protonation states were assigned
496 to titratable peptide residues together with charged N-terminus and amidated C-terminus. The peptide was placed
497 such that its centre of mass was 3.5 nm from the midplane of a rectangular lipid bilayer patch consisting of 120 1-
498 palmitoyl-2-oleoyl-sn-glycero-3-phosphoethanolamine (POPE) and 60 1-palmitoyl-2-oleoyl-sn-glycero-3-(phospho-
499 rac-(1-glycerol)) (POPG) molecules, and its helical axis was oriented parallel to the membrane. A random peptide
500 rotation angle along the helical axis was assigned and two additional transformations by 120 and 240 degrees, respec-
501 tively, were generated, resulting in three independent starting structures, each with different peptide side facing the
502 membrane. A rectangular simulation box providing 1.5 nm of solvent margins on both membrane sides was filled
503 with water molecules together with K^+ and Cl^- ions, whose number was chosen to achieve 0.15 mol/l concentration
504 and to neutralise the total system charge. The fully atomistic CHARMM36 force field [54] was used for protein and
505 ions, and the rigid TIP3P model [55] was used for water. All simulations were carried out using the Gromacs pro-
506 gram [56] with the default simulation set up implemented in CHARMM-GUI for the chosen force field combination
507 and periodic boundary conditions [57]. The protocol included potential energy minimisation, six rounds of equili-
508 bration with step-wise removal of positional restraints for peptide and lipids, and production runs. The latter were

509 conducted at ambient pressure and temperature of 310 K for 500 ns. Three independent simulations with individual
510 starting structures were performed for each peptide-membrane system. The stability of peptides α -helical structure
511 was assessed by the DSSP program [58].

512 **Data and code availability**

513 The HydrAMP source code, data used for training, and the scripts for generation of the results can be found at
514 <https://github.com/szczurek-lab/hydramp>. Free web-service is available with all the functionalities
515 can be accessed at <https://hydramp.mimuw.edu.pl/>.

516 **References**

- 517 [1] US Department of Health, Human Services, et al. “CDC. Antibiotic Resistance Threats in the United States,
518 2019”. In: *Atlanta, GA, USA: US Department of Health and Human Services, CDC* (2019).
- 519 [2] Jim O’Neill. “Tackling drug-resistant infections globally: final report and recommendations”. In: (2016).
- 520 [3] Maria Magana et al. “The value of antimicrobial peptides in the age of resistance”. In: *The Lancet Infectious
521 Diseases* (2020).
- 522 [4] Lloyd Czaplewski et al. “Alternatives to antibiotics—a pipeline portfolio review”. In: *The Lancet infectious
523 diseases* 16.2 (2016), pp. 239–251.
- 524 [5] Håvard Jenssen, Pamela Hamill, and Robert EW Hancock. “Peptide antimicrobial agents”. In: *Clinical micro-
525 biology reviews* 19.3 (2006), pp. 491–511.
- 526 [6] Chenkai Li et al. “AMPlify: attentive deep learning model for discovery of novel antimicrobial peptides effec-
527 tive against WHO priority pathogens”. In: (Dec. 2020). DOI: 10.21203/rs.3.rs-120780/v1.
- 528 [7] Qinze Yu et al. “HMD-AMP: Protein Language-Powered Hierarchical Multi-label Deep Forest for Annotating
529 Antimicrobial Peptides”. In: *arXiv preprint arXiv:2111.06023* (2021).
- 530 [8] Daniel Veltri, Uday Kamath, and Amarda Shehu. “Deep learning improves antimicrobial peptide recognition”.
531 In: *Bioinformatics* 34.16 (2018), pp. 2740–2747.
- 532 [9] Ernest Y Lee et al. “Mapping membrane activity in undiscovered peptide sequence space using machine learn-
533 ing”. In: *Proceedings of the National Academy of Sciences* 113.48 (2016), pp. 13588–13593.

- 534 [10] Patrick Timmons and Chandralal Hewage. “HAPPENN is a novel tool for hemolytic activity prediction for
535 therapeutic peptides which employs neural networks”. In: *Scientific Reports* 10 (July 2020), p. 10869. DOI:
536 10.1038/s41598-020-67701-3.
- 537 [11] Fabien Plisson, Obed Ramirez, and Cristina Martinez-Hernández. “Machine learning - guided discovery and
538 design of non-hemolytic peptides-annotated”. In: *Scientific Reports* 10 (Oct. 2020). DOI: 10.1038/s41598-
539 020-73644-6.
- 540 [12] Jacob Witten and Zack Witten. “Deep learning regression model for antimicrobial peptide design”. In: *BioRxiv*
541 (2019), p. 692681.
- 542 [13] Scott N. Dean et al. “PepVAE: Variational Autoencoder Framework for Antimicrobial Peptide Generation and
543 Activity Prediction”. In: *Frontiers in Microbiology* 12 (2021), p. 2764. ISSN: 1664-302X. DOI: 10.3389/
544 fmicb.2021.725727. URL: <https://www.frontiersin.org/article/10.3389/fmicb.2021.725727>.
- 545 [14] Ernest Lee et al. “Mapping membrane activity in undiscovered peptide sequence space using machine learning”.
546 In: *Proceedings of the National Academy of Sciences of the United States of America* 113 (Nov. 2016). DOI:
547 10.1073/pnas.1609893113.
- 548 [15] Marlon H. Cardoso et al. “Computer-Aided Design of Antimicrobial Peptides: Are We Generating Effective
549 Drug Candidates?” In: *Frontiers in Microbiology* 10 (2020), p. 3097. ISSN: 1664-302X. DOI: 10.3389/
550 fmicb.2019.03097. URL: <https://www.frontiersin.org/article/10.3389/fmicb.2019.03097>.
- 551 [16] Christina Wang, Sam Garlick, and Mire Zloh. “Deep Learning for Novel Antimicrobial Peptide Design”. In:
552 *Biomolecules* 11.3 (2021), p. 471.
- 553 [17] Jeanne Trinquier et al. “Efficient generative modeling of protein sequences using simple autoregressive mod-
554 els”. In: *arXiv preprint arXiv:2103.03292* (2021).
- 555 [18] Marwin HS Segler et al. “Generating focused molecule libraries for drug discovery with recurrent neural net-
556 works”. In: *ACS central science* 4.1 (2018), pp. 120–131.
- 557 [19] Mari Yoshida et al. “Using evolutionary algorithms and machine learning to explore sequence space for the
558 discovery of antimicrobial peptides”. In: *Chem* 4.3 (2018), pp. 533–543.

-
- 561 [20] Kyle Boone et al. “Combining genetic algorithm with machine learning strategies for designing potent antimicrobials peptides”. In: *BMC Bioinformatics* 22 (May 2021). DOI: 10.1186/s12859-021-04156-x.
- 562
- 563 [21] William Porto et al. “In silico optimization of a guava antimicrobial peptide enables combinatorial exploration for peptide design”. In: *Nature Communications* 9 (Apr. 2018). DOI: 10.1038/s41467-018-03746-3.
- 564
- 565 [22] William F Porto et al. “Joker: An algorithm to insert patterns into sequences for designing antimicrobial peptides”. In: *Biochimica et Biophysica Acta (BBA)-General Subjects* 1862.9 (2018), pp. 2043–2052.
- 566
- 567 [23] David Weininger. “SMILES, a chemical language and information system. 1. Introduction to methodology and encoding rules”. In: *Journal of Chemical Information and Computer Sciences* 28.1 (1988), pp. 31–36. DOI: 10.1021/ci00057a005. eprint: <https://pubs.acs.org/doi/pdf/10.1021/ci00057a005>. URL: <https://pubs.acs.org/doi/abs/10.1021/ci00057a005>.
- 568
- 569
- 570
- 571 [24] Donatas Repecka et al. “Expanding functional protein sequence spaces using generative adversarial networks”. In: *Nature Machine Intelligence* 3.4 (2021), pp. 324–333.
- 572
- 573 [25] Andrejs Tucs et al. “Generating ampicillin-level antimicrobial peptides with activity-aware generative adversarial networks”. In: *ACS omega* 5.36 (2020), pp. 22847–22851.
- 574
- 575 [26] Scott Dean and Scott Walper. “Variational Autoencoder for Generation of Antimicrobial Peptides”. In: *ACS Omega* XXXX (Aug. 2020). DOI: 10.1021/acsomega.0c00442.
- 576
- 577 [27] Colin M Van Oort et al. “AMPGAN v2: Machine Learning-Guided Design of Antimicrobial Peptides”. In: *Journal of Chemical Information and Modeling* (2021).
- 578
- 579 [28] Payel Das et al. “Pepcvae: Semi-supervised targeted design of antimicrobial peptide sequences”. In: *arXiv preprint arXiv:1810.07743* (2018).
- 580
- 581 [29] Payel Das et al. “Accelerated antimicrobial discovery via deep generative models and molecular dynamics simulations”. In: *Nature Biomedical Engineering* 5.6 (2021), pp. 613–623.
- 582
- 583 [30] David Eisenberg, Robert M Weiss, and Thomas C Terwilliger. “The helical hydrophobic moment: a measure of the amphiphilicity of a helix”. In: *Nature* 299.5881 (1982), pp. 371–374.
- 584

- 585 [31] Igor Zelezetsky and Alessandro Tossi. “Alpha-helical antimicrobial peptides—Using a sequence template to
586 guide structure–activity relationship studies”. In: *Biochimica et Biophysica Acta (BBA) - Biomembranes* 1758.9
587 (2006). Membrane Biophysics of Antimicrobial Peptides, pp. 1436–1449. ISSN: 0005-2736. DOI: <https://doi.org/10.1016/j.bbamem.2006.03.021>. URL: <https://www.sciencedirect.com/science/article/pii/S0005273606001088>.
- 589
- 590 [32] Eric Jang, Shixiang Gu, and Ben Poole. *Categorical Reparameterization with Gumbel-Softmax*. 2017. arXiv:
591 1611.01144 [stat.ML].
- 592 [33] Ashish Vaswani et al. *Attention Is All You Need*. 2017. arXiv: 1706.03762 [cs.CL].
- 593 [34] Nicki Skafte Detlefsen, Søren Hauberg, and Wouter Boomsma. “What is a meaningful representation of protein
594 sequences?” In: *ArXiv abs/2012.02679* (2020).
- 595 [35] John Jumper et al. “Highly accurate protein structure prediction with AlphaFold”. In: *Nature* 596.7873 (2021),
596 pp. 583–589.
- 597 [36] Sam Clark et al. “The lexicon of antimicrobial peptides: a complete set of arginine and tryptophan sequences”.
598 In: *Communications biology* 4.1 (2021), pp. 1–14.
- 599 [37] Alex Bateman et al. “UniProt: the universal protein knowledgebase in 2021”. In: *Nucleic Acids Research*
600 (2020).
- 601 [38] Jhih-Hua Jhong et al. “dbAMP: an integrated resource for exploring antimicrobial peptides with functional
602 activities and physicochemical properties on transcriptome and proteome data”. In: *Nucleic acids research*
603 47.D1 (2019), pp. D285–D297.
- 604 [39] Xinyue Kang et al. “DRAMP 2.0, an updated data repository of antimicrobial peptides”. In: *Scientific data* 6.1
605 (2019), pp. 1–10.
- 606 [40] Weizhong Li, Lukasz Jaroszewski, and Adam Godzik. “Tolerating some redundancy significantly speeds up
607 clustering of large protein databases”. In: *Bioinformatics* 18.1 (2002), pp. 77–82.
- 608 [41] Limin Fu et al. “CD-HIT: accelerated for clustering the next-generation sequencing data”. In: *Bioinformatics*
609 28.23 (2012), pp. 3150–3152.
- 610 [42] Sepp Hochreiter and Jürgen Schmidhuber. “Long short-term memory”. In: *Neural computation* 9.8 (1997),
611 pp. 1735–1780.

-
- 612 [43] Francois Chollet et al. *Keras*. 2015. URL: <https://github.com/fchollet/keras>.
- 613 [44] Zhiting Hu et al. “Toward controlled generation of text”. In: *arXiv preprint arXiv:1703.00955* (2017).
- 614 [45] Irina Higgins et al. “beta-vae: Learning basic visual concepts with a constrained variational framework”. In:
615 (2016).
- 616 [46] Diederik P Kingma and Max Welling. “Auto-encoding variational bayes”. In: *arXiv preprint arXiv:1312.6114*
617 (2013).
- 618 [47] Diederik P Kingma and Jimmy Ba. “Adam: A method for stochastic optimization”. In: *arXiv:1412.6980* (2014).
- 619 [48] Partha Ghosh et al. *From Variational to Deterministic Autoencoders*. 2019. arXiv: 1903.12436 [cs.LG].
- 620 [49] Jakub Tomczak and Max Welling. “VAE with a VampPrior”. In: *International Conference on Artificial Intelli-*
621 *gence and Statistics*. PMLR. 2018, pp. 1214–1223.
- 622 [50] Karl Pearson F.R.S. “LIII. On lines and planes of closest fit to systems of points in space”. In: *The London,*
623 *Edinburgh, and Dublin Philosophical Magazine and Journal of Science* 2.11 (1901), pp. 559–572. DOI: 10.
624 1080/14786440109462720.
- 625 [51] D Eisenberg et al. “Analysis of membrane and surface protein sequences with the hydrophobic moment plot”.
626 In: *Journal of molecular biology* 179.1 (1984), pp. 125–142.
- 627 [52] Dassault Systèmes BIOVIA. “Discovery Studio, version 21.1. 0”. In: *San Diego: Dassault Systèmes* (2021).
- 628 [53] Sunhwan Jo et al. “CHARMM-GUI: a web-based graphical user interface for CHARMM”. In: *Journal of*
629 *computational chemistry* 29.11 (2008), pp. 1859–1865.
- 630 [54] Jeffery B. Klauda et al. “Update of the CHARMM All-Atom Additive Force Field for Lipids: Validation on Six
631 Lipid Types”. In: *J. Phys. Chem. B* 114.23 (June 2010), pp. 7830–7843. ISSN: 1520-6106. DOI: 10.1021/
632 jp101759q. URL: <https://pubs.acs.org/doi/10.1021/jp101759q>.
- 633 [55] William L. Jorgensen et al. “Comparison of simple potential functions for simulating liquid water”. In: *J.*
634 *Chem. Phys.* 79.2 (1983), pp. 926–935. ISSN: 00219606. DOI: 10.1063/1.445869. URL: <http://scitation.aip.org/content/aip/journal/jcp/79/2/10.1063/1.445869%7B%5C%7D5Cnhttp://link.aip.org/link/?JCPA6/79/926/1>.

-
- 637 [56] Mark James Abraham et al. “Gromacs: High performance molecular simulations through multi-level parallelism from laptops to supercomputers”. In: *SoftwareX* 1-2 (2015), pp. 19–25. DOI: 10.1016/j.softx.
638
639 2015.06.001.
- 640 [57] Jumin Lee et al. “CHARMM-GUI input generator for NAMD, GROMACS, AMBER, OpenMM, and
641 CHARMM/OpenMM simulations using the CHARMM36 additive force field”. In: *Journal of chemical theory
642 and computation* 12.1 (2016), pp. 405–413.
- 643 [58] Wolfgang Kabsch and Christian Sander. “Dictionary of protein secondary structure: Pattern recognition of
644 hydrogen-bonded and geometrical features”. In: *Biopolymers* 22.12 (Dec. 1983), pp. 2577–2637. DOI: 10.
645 1002/bip.360221211. arXiv: 83/122577-6 [0006-3525]. URL: <http://onlinelibrary.wiley.com/doi/10.1002/bip.360221211/abstract> % 7B % 5C % %7D5Cn<http://onlinelibrary.wiley.com/doi/10.1002/bip.360221211/full%7B%5C%%7D5Cn> % 7D5Cnhttp://
646 <http://onlinelibrary.wiley.com/store/10.1002/bip.360221211/asset/360221211%7B%5C%7D5Cn> ftp.pdf?v=1%7B%5C&%7Dt=hot47ujz%7B%5C&%7Ds=8927fb6c2450d37cf0a3.
- 647
648
649

650 **Acknowledgments**

651 This work was supported by the OPUS grant no. 2019/33/B/NZ2/00956 to ES from the National Science Centre,
652 Poland, <https://www.ncn.gov.pl/?language=en>.

653 **5 Author contributions**

654 PSz., M.Mo. T.G. and E.S. conceived the project and methodology. PSz. curated the data. PSz., M.Mo. and
655 T.G. implemented the model. PSz. performed the computational analysis. M.B., W.K., and D.N. performed wet lab
656 experiments. M. Mi. and P.Se. performed computer simulations and resulting summaries of the novel peptides. J.S.
657 and T.G. created the web service. PSz. and M.Mi. prepared the figures. E.S. supervised the study. PSz., M.Mo, and
658 E.S. wrote the manuscript, with contributions and critical feedback from all authors.

659 **6 Competing interests**

660 Other projects in Ewa Szczerk's lab are cofunded by Merck Healthcare. Otherwise we do not declare other competing
661 interests.

Sequence	$\mathbb{P}_{M_{AMP}}(p)$	$\mathbb{P}_{M_{MIC}}(p)$	MIC <i>E. coli</i> ATCC 43927 [$\mu\text{g/mL}$]	MIC <i>E. coli</i> ATCC 25922 [$\mu\text{g/mL}$]
GIGKFLKKAKKFGKAFVKILKK-NH2 (Pexiganan)	0.99	0.99	4	4
GIGKFLKFALKKGLGLVLFKL-NH2	0.99	0.99	16	16
GVGKKLWFALKPLGLVKFFKLL-NH2* (Hydraganan)	0.99	0.99	2	2
GVAKKLWIAAKKPAGAGSKFKLL-NH2	0.99	0.87	512	>512
GELKKLWQAGKLSEEDGGAFKAG-NH2*	0.07	<0.01	>512	>512
FLPLIGRVLSGIL-NH2 (Temporin-A)	0.99	<0.01	256	256
FLPLIGR VFSGIL-NH2	0.99	<0.01	512	512
FLPLIGR VFSGIK-NH2	0.99	0.97	>512	>512
FLPLIGRVLSGIA-NH2	0.99	0.01	512	512
FLPLIGR VKGSIK-NH2	0.99	0.99	>512	>512
FLPIKNRYASAAE-NH2	0.08	<0.01	>512	>512

Table 1 Pexiganan and Temporin-A analogues obtained in the analogue generation process. Each row corresponds to a single peptide. $\mathbb{P}_{M_{AMP}}(p)$ is a probability of a given peptide being an AMP. $\mathbb{P}_{M_{MIC}}(p)$ is a probability of a given peptide being active. Minimal Inhibitory Concentration (MIC) values ($\mu\text{g/mL}$) were measured against reference strains of microorganisms (*E. coli* ATCC 43927, *E. coli* ATC 25922). Peptides in bold were experimentally proven to show activity in accordance with Classifier prediction. Peptide whose sequences are marked with an asterisk were subjected to molecular dynamics simulations.

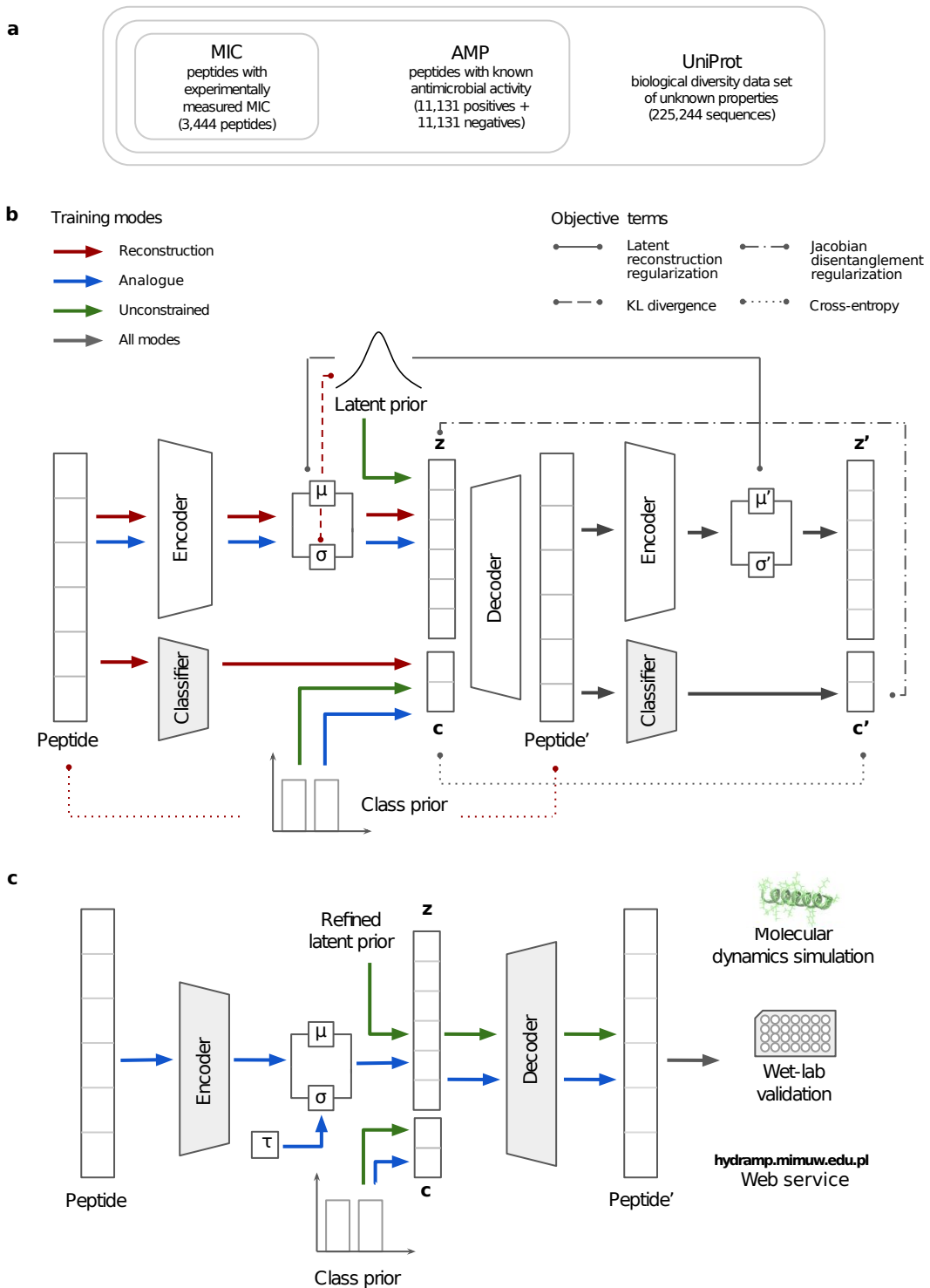


Fig. 1 HydrAMP architecture and data traversal overview.

Fig. 1 Continued caption. **a** Compositional structure of the training data set. **b** Data flow and optimization setup during training. Colors indicate training modes and show the path each peptide traverses within a mode. Line styling indicates the objective terms. Shaded areas indicate components with frozen weights. **c** Data flow during generation. In the final step molecular dynamics simulation and wet-lab validation are performed. HydrAMP functionality is available via a web service <https://hydramp.mimuw.edu.pl/>.

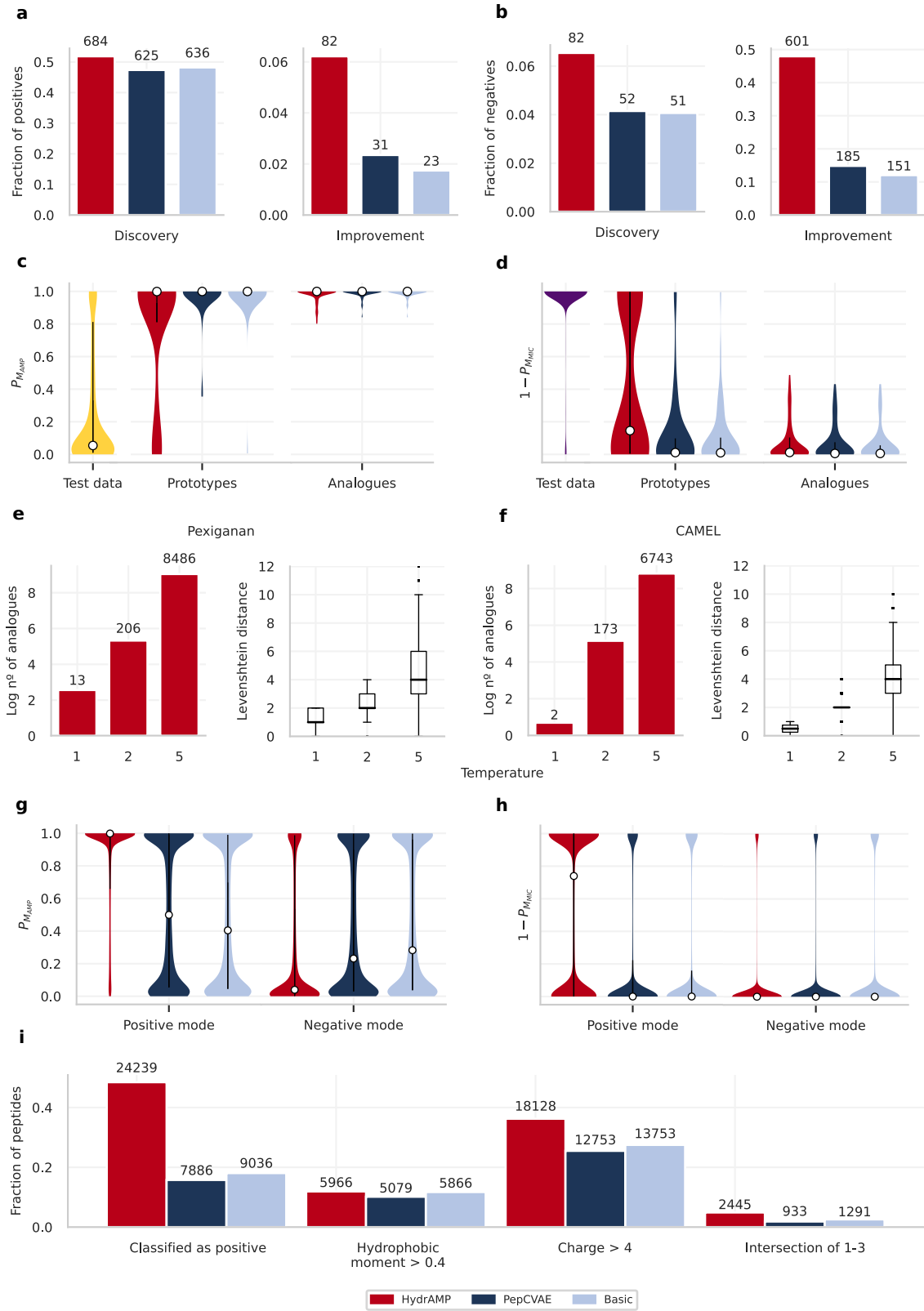


Fig. 2 Generative performance of HydrAMP (red), in comparison to PepCVAE (dark blue), and Basic (light blue).

Fig. 2 Continued caption. **a** Fraction (y-axis) and number (over each bar) of 1319 positive (AMP and highly active) peptides from the test set (y-axis), that produced analogues that met discovery or improvement criteria (x-axis) in the analogue generation. **b** As in **a**, but for 1253 negative peptides from the test set. **c** The distribution of the probability of being AMP for 1253 negative prototypes and their analogues that met the discovery criteria, compared to the distribution for the test data (yellow). **d** The distribution of probabilities of not being highly active ($1 - \mathbb{P}_{M_{MIC}}$) for 1253 negative prototypes and their analogues that met the discovery criteria, compared to the distribution for the test data (violet). **e, f** Left: The relation between the creativity parameter *temperature* (x-axis) and the log number of generated unique analogues that met the discovery criteria, out of 10k attempts (y-axis; the actual number of analogues shown above each bar). Right: the distribution of the Levenshtein distances between generated analogues and the prototype sequence of Pexiganan (**e**) and CAMEL (**f**) AMPs. **g** Probability of being antimicrobial ($\mathbb{P}_{M_{AMP}}$) for 50,000 peptides generated in unconstrained mode, for both positive and negative modes (x-axis). **h** The distribution of probabilities of not being highly active ($1 - \mathbb{P}_{M_{MIC}}$) for 50,000 peptides generated in unconstrained mode for both positive and negative modes. In panels **c, d, g, h**, the white dots mark the median of each distribution. **i** Fraction of 50,000 peptides generated in the unconstrained positive mode classified as positives (first bar plot), fraction of peptides have hydrophobic moment > 0.4 (second bar plot), fraction of peptides with charge > 4 (third bar plot) and fraction of peptides that satisfy all previous criteria: classified as positive, high hydrophobic moment, and high charge (fourth bar plot). The number over each bar: the actual number of peptides with the condition.

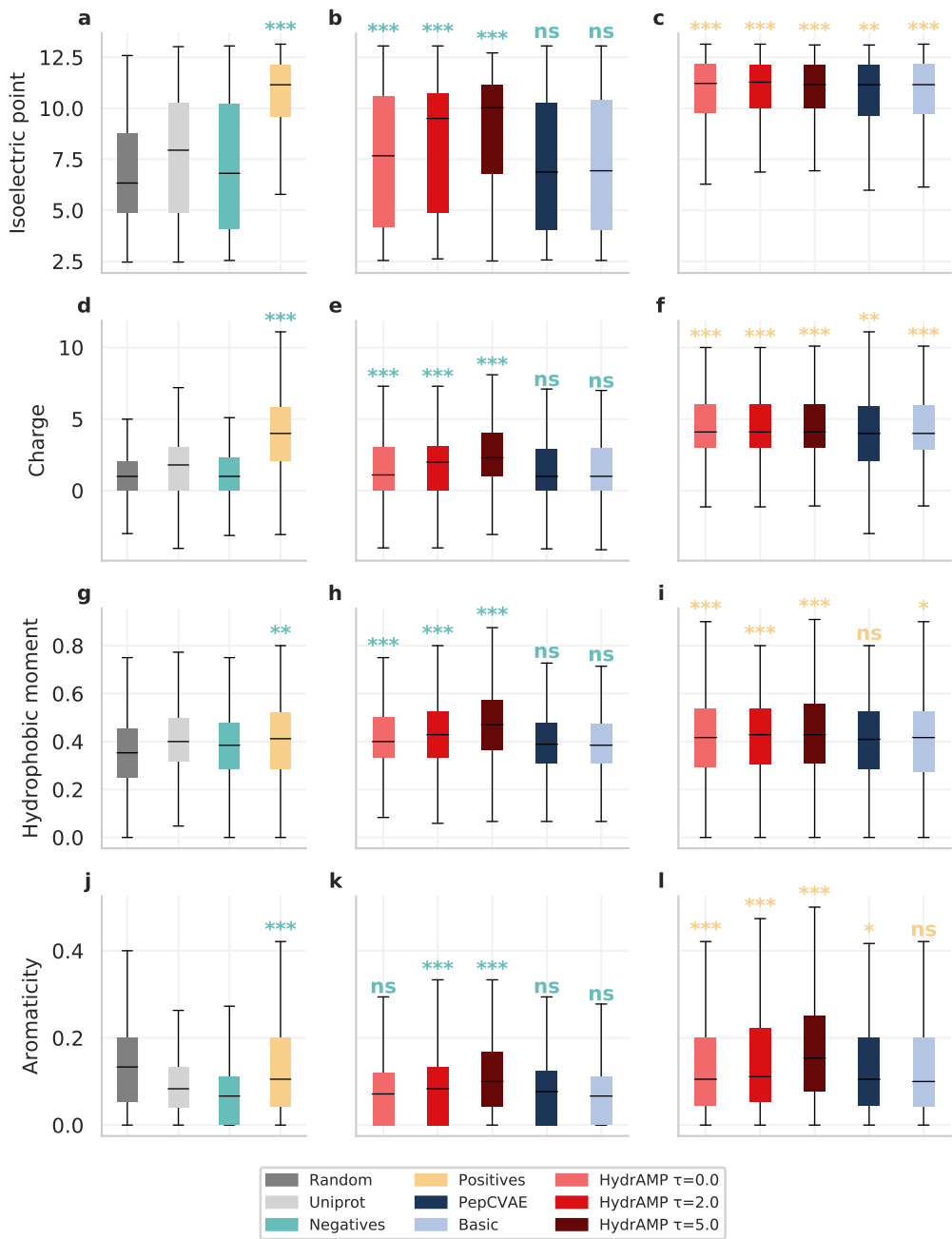


Fig. 3 Physicochemical properties of analogues generated by HydrAMP and compared methods in analogue generation mode for non-AMP or AMP templates in comparison with real and random data. Boxplots of properties (a, b, c) Isoelectric point, (d, e, f) Charge, (g, h, i) Hydrophobic moment, (j, k, l) Aromaticity) of randomly generated peptides (dark gray), peptides sampled from UniProt (light gray), true negatives (green), and true positives (yellow), in comparison with AMP analogues generated from negatives (b, e, h, k), and positives (c, f, i, l) improved by different models: HydrAMP with various creativity parameter *temperature* values: $\tau = 1.0$ (light red), $\tau = 2.0$ (red), $\tau = 5.0$ (dark red), PepCVAE (dark blue), Basic (light blue). Significance levels are denoted as: ns - $P \geq 0.05$; * - $P \leq 0.05$; ** - $P \leq 0.01$; *** - $P \leq 0.001$.

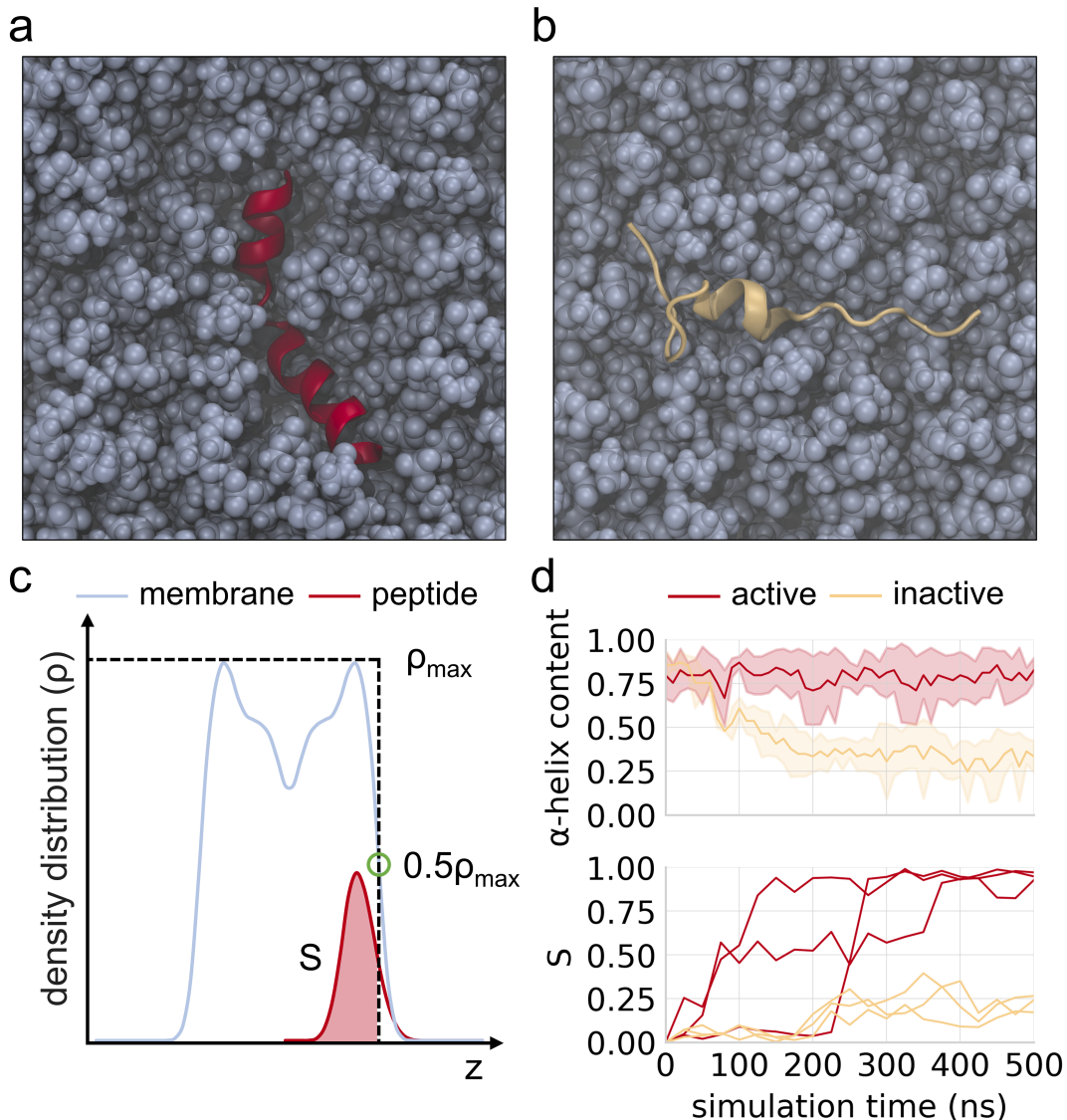


Fig. 4 Summary of atomistic molecular dynamics simulations of active antimicrobial peptide Hydraganan and experimentally verified non-AMP peptide within a model bacterial lipid membrane. **a, b**, late simulation snapshots of active (red) and inactive (beige) peptides, respectively, in the membrane (blue); a top view on membrane surface; water molecules not depicted for clarity; **c**, a scheme illustrating the evaluation of the S parameter describing the level of peptide burial within the membrane; z – membrane normal axis; **d**, upper plot: an average (lines) and standard deviation (shaded areas) of alpha helix fraction within peptide residues; lower plot: the evolution of S parameter for each of three initial peptide placements.